5th INTERNATIONAL SCIENTIFIC CONFERENCE
ON DEFENSIVE TECHNOLOGIES
OTEH 2012
Belgrade, Serbia, 18 – 19 September 2012

STRESS CORROSION CRACKING OF AN AL-ZN-MG-CU ALLOY AFTER DIFFERENT PRECIPITATION HARDENING TREATMENTS

ANA ALIL
Institute GOŠA, Belgrade, ana.alil@institutgosa.rs

BORE JEGDIĆ
Institute GOŠA, Belgrade, bore.jegdic@institutgosa.rs

BILJANA BOBIĆ
Institute GOŠA, Belgrade, biljana.bobic@institutgosa.rs

MIROSLAV RADOSAVLJEVIĆ
Institute GOŠA, Belgrade, miroslav.radovanovic@institutgosa.rs

BORIS KATAVIĆ
Institute GOŠA, Belgrade, boris.katavic@institutgosa.rs

Abstract: *Stress corrosion cracking (SCC) was tested in a high strength 7000 series aluminium alloy applied for weapons and military equipment. The effect of one step- and two-step precipitation hardening (aging) on SCC was investigated. The slow strain rate test (SSRT) and the fracture mechanics (FM) method were used for SCC testing. The measurements of electrical resistivity allowed evaluating an aging degree in the tested alloy. Both testing methods have shown that the alloy after two-step precipitation hardening is significantly more resistant to SCC. The critical stress intensity factor for SCC, K_{ISCC} is significantly higher, and the crack growth rate on the plateau, v_{pl} is more than one order of magnitude lower for the alloy in this state. Processes that take place at the crack tip are proposed and the effect of copper was analyzed. The effect of the testing solution (NaCl) temperature on the v_{pl} was determined. Two values of the apparent activation energy, E_a, were obtained; one value (46.6 kJ mol^{-1}) refers to higher temperatures, while the other (70.4 kJ mol^{-1}) refers to lower test temperatures. These values of E_a correspond to the different processes that control the v_{pl}, at higher and lower temperatures.*

Key words: *aluminium alloys, stress corrosion cracking, fracture mechanics, slow strain rate test.*

1. INTRODUCTION

Stress corrosion cracking (SCC) is a time-dependent process that occurs under the influence of residual or imposed tensile stress and specific corrosion environment. Localized corrosion (intergranular, pitting) usually proceeds to the SCC. Mechanical damage on the surface may play the role of an initial crack [1]. In general, the following three conditions have to be fulfilled for SCC to occur: (1) the alloy is prone to SCC; (2) the alloy is in a specific corrosion environment and (3) the value of tensile stress is higher than the threshold value [2]. According to fracture mechanics (FM), the third condition is defined so that the coefficient of the stress intensity on the crack tip K_I is higher than some critical value K_{ISCC} [3].

The 7000 series aluminium alloys (Al-Zn-Mg-Cu) have maximum strength but they are prone to SCC. However, the tendency of these alloys to SCC changes depending on the content of alloying elements, mechanical, thermal and thermo-mechanical treatment [3-6]. The precipitation hardening of the 7000 series aluminium alloys takes place through the segregation of GP zones that are transformed through the intermediate η' phase into the equilibrium phase $MgZn_2$ [7-10]. The maximum strength is achieved in the structure where there is a mixture of GP zones and η' precipitates. But in the state of maximum strength the alloy is prone to SCC. In the over-aged state (T73) the alloy is characterized with a good resistance towards both SCC and exfoliation corrosion. In the partially over-aged state (T76), the alloy shows a slightly lower resistance to SCC and high resistance to exfoliation corrosion, while in the state of maximum strength (T6) the alloy is sensitive to both types of corrosion [1, 7, 10, 11].

The 7000 series aluminium alloys not intended for welding contain copper. The addition of copper has a beneficial effect on hardness, increasing the volume fraction of the hardening precipitates. It was found that copper is incorporated in the GP zones, making them more stable even at higher temperatures [7, 12]. In addition, copper atoms replace zinc atoms in the hardening precipitate η' ($MgZn_2$), particularly at temperatures above 150 °C [12, 13], making the precipitate nobler. All this provide conditions for the increased resistance of these alloys to SCC.

The 7000 series aluminium alloys in the over-aged state achieved by two-stage aging are characterized by high resistance to SCC and exfoliation corrosion. However, the aging time is relatively long, and the hardness of the alloys is significantly reduced (~ 15% compared to the state of maximum hardness). Based on the results reported [3, 5, 7], a two-stage aging process was proposed. This process is performed in a short period of time. The tensile properties of the alloys in this state remain unchanged compared to the state of maximum hardness. The electrochemical and SCC characteristics of the alloy in the state of maximum hardness as well as in the state after two-aging process were investigated in this study. In addition, SCC tests at different temperatures were done in a 3.5 wt. % NaCl solution and the apparent activation energies were obtained. According to Helroyd and Scamans [14], the stress corrosion crack growth rate v_{pl} at temperatures below ~ 40°C has apparent activation energy, highly dependent on copper content. No copper content dependency was observed at temperatures above ~40°C. The influence of temperature at the kinetic of the stress corrosion crack growth is of great practical importance, because a large number of SCC processes take place at increased temperatures.

2. EXPERIMENTAL PART

2.1. Materials

The chemical composition of the tested alloy is given in Table 1. The test samples were cut from pressed rods (80x30 mm). The rods were obtained by continuous casting of billets and then subjected to homogenization annealing at 465°C/18h.

Table 1. Chemical composition of the Al-Zn-Mg-Cu alloy (wt. %):

Zn	Mg	Cu	Mn	Cr	Zr	Al
7.2	2.15	1.46	0.28	0.16	0.12	Rest

The heat treatment of the samples was performed according to the following regimes:

– Homogenization annealing at 460°C/1h, quenching in water at room temperature, then precipitation hardening at 120°C/24h (one-stage aging, indicated in this paper with TA).

– Homogenization annealing at 460°C/1h, quenching in water at room temperature, precipitation hardening at 100°C/5h, and then at 160°C/5h (two-stage aging, indicated in this paper with TB).

The tensile characteristics of the tested aluminium alloy after heat treatment are listed in Table 2.

Table 2. Tensile characteristics of the Al-Zn-Mg-Cu alloy

Thermal State	$R_{p0.2}$ (MPa)	R_m (MPa)	A_5 (%)
TA	560	620	10.5
TB	570	600	9.5

2.2. Measurement of electrical resistivity

The measurements were performed on the TA and TB samples. The method of measurement is described in ASTM B193 standard. Electrical resistivity was measured by a microohmmeter in accordance with the manufacturer's instructions. The value of the measured electrical resistivity (ρ) was recalculated into electrical conductivity (χ=1/ρ), as well as into the IACS% factor, using the equation:

$$IACS = \frac{\chi}{\chi_{Cu}} \times 100\% \tag{1}$$

Where: χ is the value of the electrical conductivity of the tested alloy, and χ_{Cu} is the electrical conductivity of pure copper (58.34 MS m^{-1}).

2.3. Slow strain rate test (SSRT)

The susceptibility to SCC was determined by the SSRT method. The elongation to fracture obtained during the testing of identical samples in the corrosion environment and in the air enabled the calculation of the index of tendency to SCC (I_{SCC}):

$$I_{SCC} = 1 - \frac{A_{SCC}}{A_0} \tag{2}$$

Where: A_{SCC} - elongation in the corrosion environment, A_0 – elongation in the air.

For an alloy resistant to SCC in a given corrosion environment, the value of $I_{SCC} \rightarrow 0$, and for the alloy prone to SCC the value of $I_{SCC} \rightarrow 1$ [15].

There is a critical interval of the initial strain rates where SCC occurs. To perform the test a value of the initial strain rate from the critical interval was chosen and all subsequent tests were performed at the chosen strain rate. The test specimens were of a circular cross section (ϕ6 mm) and of 30 mm working length (ASTM E8). Before the test, the dimensions of the specimens were carefully measured. Then the specimens were degreased with ethanol and placed in the cell for testing SCC. The tests were done on the "Instron" tensile machine in the air at the standard initial strain rate and in the corrosion environment (2 wt. % NaCl + 0.5 wt. % Na_2CrO_4, pH3). In this case, the initial strain rate was 6.94 10^{-6} s^{-1}. Data needed for the calculation of the I_{SCC} were taken from the obtained curve strain-deformation.

2.4. Fracture mechanics (FM) method

A bolt-loaded double-cantilever-beam (DCB) test specimen was chosen for testing SCC by the FM methodology. The samples were cut in the S-L orientation since aluminium alloys are most sensitive to SCC at this orientation (force action in the short transverse direction).

The thickness of the sample (*B*) was calculated based on the known fracture toughness (K_{IC}) and the yield strength ($R_{0.2}$) of the alloy, using the equation:

$$B = \min 2.5\, (K_{IC} / R_{0.2})^2 \tag{3}$$

The other dimensions of the DCB sample were determined in the dependence on the sample thickness (*B*=25 mm). The starting value of the K_{I0} was calculated on the basis of the measured value of the crack length (*a*), the sample half-height (*H*) and the given size of the crack opening on the line of the load (V_Y), according to the following equation [ISO 7539-6]:

$$K_{I0} = \frac{E \cdot V_Y \cdot H \cdot \sqrt{3H(a+0{,}6H)^2 + H^3}}{4\left[(a+0{,}6H)^3 + H^2 a\right]} \tag{4}$$

The starting crack was formed mechanically on the sample [16], and the crack length was precisely measured. The SCC testing was done in accordance with the procedure described [7] in a 3.5 wt. % NaCl solution. The increase of the crack length was measured microscopically in the next 150 days. The diagram of time dependence of the crack length was fitted and smoothed with the appropriate curve. That curve is used for calculating and drawing the diagram of the crack growth rate dependence on the K_I. At the end of the testing, a fracture of the samples was performed. On the surface of the fracture, the length of the crack formed mechanically and the total length of the mechanical and stress-corrosion crack were precisely measured. The real value of the stress intensity (that approximately suits the value of the K_{IC}) and the real value of the stress intensity when the crack practically stops, K_{ISCC}, were calculated (eq.4).

In addition, SCC tests at different temperatures were done in a 3.5 wt. % NaCl solution. The length of the crack was measured during the time and the v_{pl} was calculated for every chosen temperature.

3. RESULTS AND DISCUSSION

The tested aluminium alloy, aged according to the TA and TB regimes, is characterized with an appropriate structure, mechanical properties, corrosion resistance, electrical conductivity and electrochemical properties. Based on these indicators, the tendency of the alloy to SCC was evaluated.

3.1. Electrical resistivity

The change of the IACS factor during the second stage of aging (TB) is shown in Figure 1.

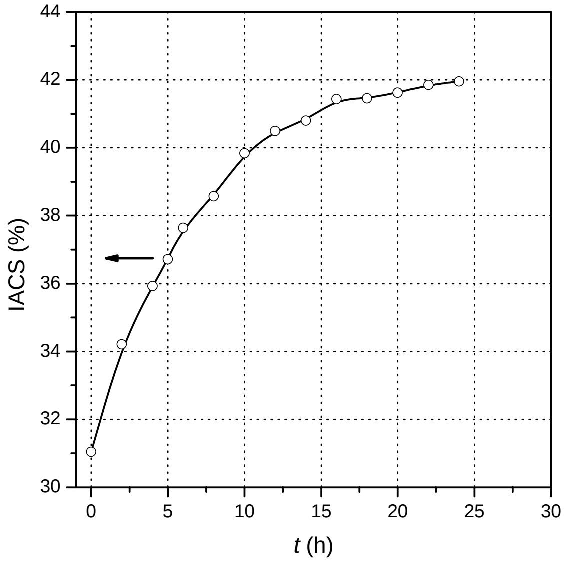

Figure 1. Change of the IACS factor during and after the second stage of the two-stage aging. The arrow signifies the end of the second stage.

The electrical resistivity and the recalculated values of electrical conductivity and the IACS% factor for TA and TB state of the tested aluminium alloy are shown in Table 3.

Table 3. Electrical resistivity and the recalculated values of electrical conductivity and the IACS factor after homogenization annealing (T0), one-stage (TA) and two-stage (TB) aging.

Thermal State	ρ (nΩ m)	χ (MS m^{-1})	IACS (%)
T0	5.82	17.20	29.65
TA	5.30	18.88	32.56
TB	4.75	21.06	36.71

The obtained results (Table 3) have shown that the TB sample has larger conductivity than the TA sample and the T0sample immediately after homogenization annealing. A supersaturated solid solution with a high concentration of vacancies was obtained after quenching. Fields of elastic strains around vacancies cause dissipation of electrons, so lower values of conductivity are obtained [17]. During aging, the clusters of zinc are formed at first, followed by the GP zones which grow gradually and transform themselves into the half-coherent phase η'. Elastic strains around the GP zones and the η' phase caused more electron dissipation, so low values of conductivity are obtained. With appearance of the stabile η phase during two-stage aging, elastic strains decrease, and the alloy conductivity increases (Figure 1). The formed precipitates get coarser (their dimensions increase while their number decreases), and conductivity still increases with a prolonged time of aging (approximately 42 IACS%, after 24 h, Figure 1). However, the mechanical characteristics of the alloy (hardness) are decreased [7], and the resistance to exfoliation corrosion and SCC is lowered. For the 7000 series aluminium alloys, the criteria of electrical conductivity for SCC and exfoliation corrosion can be found [18].

3.2. Slow strain rate tests (SSRT)

The results of the SCC testing with the SSRT method are presented in Table 4.

Table 4. Results of the SCC testing with the SSRT method at room temperature.

Thermal State	Environment	$A = \Delta l / l_0$ (%)		I_{SCC} (%)	
TA	air	8.6	9.2	-	-
		9.2		-	-
		9.8		-	-
	solution	7.0	5.6	24	39.0
		4.8		48	
		5.1		45	
TB	air	7.2	8.8	-	-
		9.4		-	-
		9.9		-	-
	solution	8.7	8.7	1	7.3
		10.3		0	
		7.0		21	

The results are obtained in a relatively short time (about 10 h for one sample) which is the basic advantage of the method compared to the FM method. Testing with the FM method lasts for several months.

The results indicate that the SSRT method is selective to the applied thermal states. It can be seen that the TB state is more resistant to SCC than the TA state. The processes of formation and growth of the crack and the final unstable fast fracture are not separated, so the data of total tendency to formation and growth of stress corrosion cracks is obtained using this method.

3.3. Fracture mechanics (FM) method

The main advantage of the FM method is getting quantitative data about alloy susceptibility to SCC (K_{ISCC}, $v = da/dt$). A diagram of dependence of the stress corrosion crack rate on the K_I is given in Figure 2.

When the K_I is smaller than the K_{ISCC}, there is no growth of the stress corrosion crack or the growth rate is too small that can be neglected. In the first stadium (I), the crack growth rate strongly depends on the K_I. In the second stadium (II), the crack growth rate practically does not depend on the K_I. The influence of the alloy heat treatment is significant and it reflects in shifting the level of the second stadium to higher or lower values (Figure 2). In the third stadium (III), v increases fast until the critical value K_{IC} is reached, when it comes to a quasi-static fracture. The results of SCC testing by the FM method are presented in Table 6.

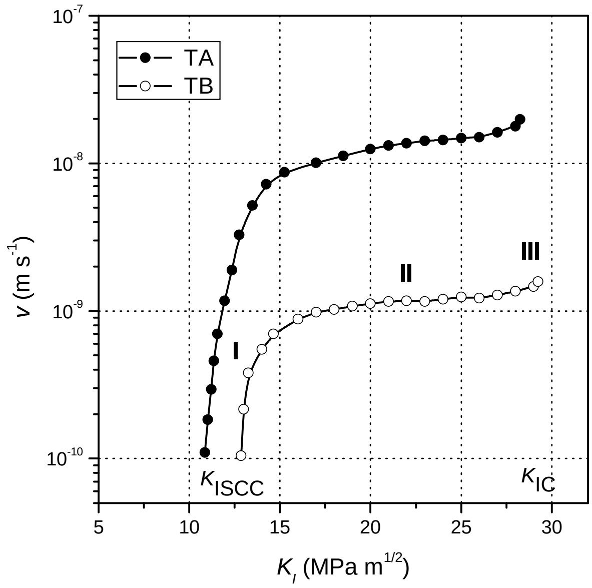

Figure 2. Influence of the heat treatment regime on the log v - K_I dependence.

It can be seen that that the alloy is more resistant to SCC after two-step aging (TB). The difference in SCC resistance is reflected on the v_{pl} value. The value of the v_{pl} is lower for more than one order of magnitude in the TB case. The structure of the tested alloy, obtained during two-step aging, is considerably more resistant to SCC than the structure obtained by one-step aging. The maximum strength of the alloy (TA state) is obtained when GP zones and η' precipitates are present in a structure. Local plastic deformation at the tip of the stress corrosion crack causes mainly planar slipping when dislocations cut GP zones and smaller particles of the η' phase. It comes to the accumulation of dislocations at the grain boundaries at the crack tip, which causes increase in local stress, so that SCC starts at lower external stress. These create favourable conditions for the SCC process to occur according to the mechanism of local hydrogen embrittlement or to the mechanism of anodic dissolution [7,9].

Table 6. Results of the SCC testing by the FM method.

Thermal State	K_{I0} (MPa m$^{1/2}$)	K_{ISCC} (MPa m$^{1/2}$)	v_{pl} (m s^{-1})
TA	28.25	10.87	14.4 10^{-9}
TB	29.25	12.87	1.16 10^{-9}

In the TB case, a great number of GP zones is created in the first stage, at a lower temperature (100°C). The smaller particles of the η' phase precipitate on the GP zones during the second stage of aging (160°C) and then they are partially transformed into the stable η phase. In this case, the local plastic deformation at the crack tip is homogeneous (so-called turbulent slipping). Dislocations cannot succeed in cutting the particles of the stable η phase and dislocations are uniformly distributed inside the grains. There is no local increase in stress at the grain boundaries and that creates favourable conditions for higher resistance to SCC [7, 9].

The influence of alloying with copper reflects in the electrochemical characteristics of the alloy structural constituents. In the Al-Zn-Mg alloys, the η phase precipitated on the grain boundary is anodic compared to the grain itself (which is covered with a passive film). These conditions are favourable for intergranular corrosion and SCC to occur. In the tested alloy, copper atoms enter into the basis (solid solution) and into the precipitates, $Mg(AlCuZn)_2$ making them nobler [11]. The precipitates on the grain boundaries are dissolved slower, and the cathodic reaction (hydrogen ion reduction) becomes more difficult [7, 11]. In the presence of copper, the GP zones are more stable at higher temperatures and the fraction of the strengthening precipitate in the alloy increases. These cause an increase in strength and resistance to SCC [7, 12, 13]. Accordingly, copper affects the mechanism of plastic deformation (slipping) and the electrochemical characteristics of the matrix and the precipitates. All this contributes to the increased SCC resistance. The influence of other factors, such as formation of magnesium hydride at the grain boundaries [8, 19, 20] and other possible mechanisms of SCC occurrence are not considered in this paper.

The influence of the test solution temperature on the v_{pl} is shown in Figure 3. The exponential increase of the v_{pl} with the increase in temperature can be noticed, which is expressed by the following equation:

$$v = v_0 \exp(-E_a/RT) \tag{5}$$

Where: E_a is the apparent activation energy of the process that controls the v_{pl}.

If the previous equation is logarithmed, a linear dependence between the logarithm of the v_{pl} and the reciprocal value of the temperature is gained (Equ. 6).

$$\ln v = \ln v_0 - E_a/RT \tag{6}$$

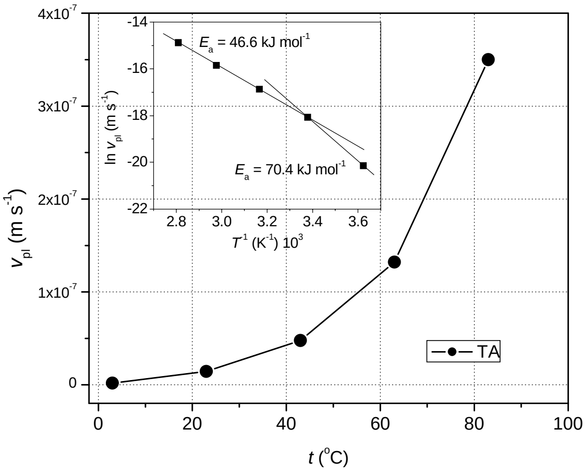

Figure 3. Temperature dependence of v_{pl} during SCC testing (TA state).

The dependence of the v_{pl} on the reciprocal value of the temperature is shown in the insert in Figure 3. From the slope of the straight line, the apparent activation energy of the process that controls the v_{pl} is obtained. There are two values of the apparent activation energy. One value (E_a = 46.6 kJmol^{-1}) refers to the temperature interval from 23 to 83°C, while the other value (E_a = 70.4 kJmol^{-1}) refers to the lower testing temperatures, from 3 to 23°C. These values of apparent activation energies correspond to different processes that control the v_{pl}. This is in accordance with the reported results [7, 14].

It was proposed that the crack propagation v_{pl} at temperatures above ~ 40°C is associated with aluminium hydride formation (E_a ~ 35 kJmol^{-1}). The decomposition of aluminium hydride within the crack-tip region leads to significantly enhanced local entry of hydrogen, which facilitates the observed increase of v_{pl}, independent of the copper content. The crack propagation v_{pl} at temperatures below ~ 40°C is dependent on the availability of hydrogen generated via the electrochemical process. The specific role of copper is not yet fully established for SCC occurrence in water vapour, distilled water and aqueous saline solutions, even at room temperature [14]. However, anodic dissolution and grain boundary slipping are clear candidate processes for regimes with apparent activation energies of 80 to 110 kJmol^{-1}.

The results obtained by the FM method have a quantitative character. In the case of real SCC danger in exploitation, the value of the K_{ISCC} should be used in the calculation of the allowed stress, instead of the K_{IC}. For the calculation of the constructions work life, the stress corrosion crack growth rate should be applied.

4. CONCLUSIONS

The corrosion and SCC resistance of a high strength 7000 series aluminium alloy (Al-Zn-Mg-Cu) was tested. The alloy was subjected to the classical one-step aging (TA) as well as a new two-step aging (TB). The testing was performed using several techniques that gave useful data related to the electrochemical behaviour, SCC and structural state of the tested alloy. It was shown that the alloy after two-step aging had considerably higher resistance to the corrosion and SCC compared to the alloy after one-step aging.

The measurements of electrical conductivity enabled the estimation of the structural state of the alloy, i.e. the type and the degree of precipitation. The resistance to the localized types of corrosion (exfoliation, pitting and SCC) depends on the presence of different phases developed during the aging process. It can be suggested that measuring electrical conductivity is the most economical method for the control of aluminium alloys products that strengthen with precipitation hardening.

The qualitative results were obtained by the SSRT method. The results indicate total resistance of the alloy to the SCC. The used method is selective considering the tested thermal states, i.e. the TB state is more resistant to the SCC than the TA state. The results were gained for a relatively short period of time which is the basic advantage of the SSRT method. The method is suitable for the development of new alloys and optimal regimes of thermal processing.

The results obtained with the FM method are of a quantitative character. The value of K_{ISCC} is higher, and the v_{pl} is lower for more than one order of magnitude for the two-step aged alloy. The explanation for the processes that take place at the crack tip during SCC of the alloy in the TA and TB states and copper influence is proposed. In the case of real SCC danger in exploitation, the value of the K_{ISCC} should be used in the calculation of the allowed stress, instead of the K_{IC}. For the calculation of the construction work life, the stress corrosion crack growth rate should be applied.

Two values of apparent activation energies have been obtained. One value (E_a = 46.6 kJmol^{-1}) refers to the temperature interval from 23 to 83^{o}C, while the other value (E_a = 70.4 kJmol^{-1}) refers to the lower temperatures, from 3 to 23^{o}C. The most likely processes that control the v_{pl} at lower and higher temperatures were suggested.

ACKNOWLEDGEMENT

This work was co-financed from the Ministry of Education of the Republic of Serbia (project No. TR 34028 and Grant No. III 45019).

Thank you Note

The authors thank the Sector for Materials and Protection, Military Technical Institute, Belgrade, for the assistance in the experimental testing of SCC.

References

[1] Jones, R.H.: *Stress-Corrosion Cracking*, in *Corrosion: Fundamentals, Testing, and Protection*, Vol 13A, ASM Handbook, ASM International, 2003, p 346–366

[2] Landolt, D.: *Corrosion and Surface Chemistry of Metals*, Lausanne, Switzerland, 2007.

[3] Herberg, R.W.: *Deformation and Fracture Mechanics of Engineering Materials,* J. W. and Sons, New York, 1983.

[4] Speidel, M.O.: *Stress Corosion Cracking of Aluminum Alloys*, Metallurgical and Materials Transactions A, 6A (1975) 631-651.

[5] Brown, B.F.: *Stress Corrosion Cracking Control Measures*, NACE, monograph 156, Ohio, 1977.

[6] Moran, J.: *Effects of Metallurgical Variables on the Corrosion of Aluminum Alloys*, in Corrosion: Fundamentals, Testing, and Protection, Vol 13A, ASM Handbook, ASM International, 2003, pp. 275–278.

[7] Fontana, M.G. and Staehle, R.W.: *Advances in Corrosion Science and Technology*, vol. 2, vol. 3 and vol. 7, Plenum Press, New York, 1972, 1973 and 1980 (Russian translation).

[8] Bobby, M., Kannan, P., Bala, S., Raja, V.S.: *Stress corrosion cracking (SCC) of aluminium alloys, in Stress corrosion cracking,* Theory and practice, Edited by: Raja, V.S. and Shoji, T., Oxford, Cambridge, Philadelphia, New Delhi, 2011, pp. 307-340.

[9] Sinjavskij, V.S., Valjkov, V.D., Kalinin, V.D.: *Korrozija i zaschita aljuminijevih splavov*, Moskva, Metalurgija, 1986.

[10] Jegdić, B.: *Behavior of Stress Corrosion Crack in a High-Strength Aluminum Alloys Structure*, Scientific-Technical Review, LIII (2003) 19-24.

[11] Summerson, T.J. and Sprowls, D.O.: *Corrosion Behavior of Aluminum Alloys*, Vol. III, Conference Proceedings, Aluminum Alloys-Physical and Mechanical Properties, Ed. Starke E. A. and Sanders, T. H., Virginia, June 1986, pp. 1576-1662.

[12] Hatch, J.E.: *Aluminum: Properties and Physical Metallurgy*, American Society for Metals, 1984.

[13] Mondolfo, L.F.: *Aluminum Alloys: Structure and Properties*, Butterworths, 1976.

[14] Henry Holroyd, N.J. and Scamans, G.M.: *Crack Propagation During Sustained-Load Cracking of Al-Zn-Mg-Cu Aluminum Alloys Exposed to Moist Air or Distilled Water*, Metallurgical and Materials Transactions A, 42A (2011) 3979-3998.

[15] Ugianski, G.M. and Payer, J.H. Ed.: *Stress Corrosion Cracking - The Slow Strain Rate Technique*, STP 665, ASTM, Philadelphia, 1979.

[16] Phull, B.: *Evaluating Stress-Corrosion Cracking, Corrosion: in Fundamentals, Testing, and Protection*, Vol 13A, ASM Handbook, ASM International, 2003, p 575–616

[17] Novikov, I.I.: *Theory of heat treatment of metals*, Mir Publishers, Moscow, 1978.

[18] Davis, J.R.: *Corrosion of Aluminum and Aluminum Alloys*, ASM International, Ohio, 1999.

[19] Young G.A. Jr. and Scully, J.R.: *The Effects of Test Temperature, Temper, and Alloyed Copper on the Hydrogen-Controlled Crack Growth Rate of an Al-Zn-Mg-(Cu) Alloy*, Metallurgical and Materials Transactions A, 43A (2002) 101-115.

[20] Burleigh, T.D.: *The Postulated Mechanisms for Stress Corrosion Cracking of Aluminum Alloys* A Review of the Literature" 1980-1989, Corrosion, 47 (1991) 89-97.